Available online at www.sciencedirect.com
SCIENCE DIRECT®
Bioelectrochemistry 63 (2004) 79–85
Bioelectrochemistry
www.elsevier.com/locate/bioelechem

Binding of single nucleotides to H^+-ATP synthases observed by fluorescence resonance energy transfer

S. Steigmiller[a], B. Zimmermann[a], M. Diez[a], M. Börsch[b], P. Gräber[a,*]

[a] *Institut für Physikalische Chemie, Albert-Ludwigs-Universität Freiburg, Albertstr. 23a, D-79104 Freiburg, Germany*
[b] *3. Physikalisches Institut, Universität Stuttgart, Germany*

Received 23 June 2003; received in revised form 11 August 2003; accepted 27 August 2003

Abstract

F_0F_1-ATP synthases couple proton translocation with the synthesis of ATP from ADP and phosphate. The enzyme has three catalytic nucleotide binding sites, one on each β-subunit; three non-catalytic binding sites are located mainly on each α-subunit. In order to observe substrate binding to the enzyme, the H^+-ATP synthase from *Escherichia coli* was labelled selectively with the fluorescence donor tetramethylrhodamine (TMR) at position T106C of the γ-subunit. The labelled enzymes were incorporated into liposomes and catalysed proton-driven ATP synthesis. The substrate ATP-Alexa Fluor 647 was used as the fluorescence acceptor to perform intermolecular fluorescence resonance energy transfer (FRET). Single molecules are detected with a confocal set-up. When one ATP-Alexa Fluor 647 binds to the enzyme, FRET can be observed. Five stable states with different intermolecular FRET efficiencies were distinguished for enzyme-bound ATP-Alexa Fluor 647 indicating binding to different binding sites. Consecutive hydrolysis of excess ATP resulted in stepwise changes of the FRET efficiency. Thereby, γ-subunit movement during catalysis was directly monitored with respect to the binding site with bound ATP-Alexa Fluor 647.

Keywords: ATP synthase; Single-molecule spectroscopy; Intermolecular FRET; Fluorescent ATP derivatives

1. Introduction

Membrane-bound H^+-ATP synthases catalyse the formation of ATP from ADP and inorganic phosphate in mitochondria, chloroplasts and bacteria. H^+-ATP synthases are multi-subunit complexes (with eight different subunits in *Escherichia coli*) and consist of two major parts (Fig. 1a). The hydrophobic membrane-integrated F_0-part with subunit composition ab_2c_{10-14} is involved in proton translocation across the membrane [1–4]. The hydrophilic F_1-part with subunit composition $\alpha_3\beta_3\gamma\delta\varepsilon$ contains three catalytic binding sites, one on each β-subunit and three non-catalytic binding sites (mainly on each α-subunit) which bind ATP, ADP and phosphate [2]. F_1 and F_0 are linked by a central stalk containing the γ- and ε-subunits, which directly interact with a ring of c-subunits [5]. A second, peripheral stalk is formed by the δ- and two b-subunits [6–8].

The three catalytic nucleotide binding sites (Fig. 1b) on the β-subunits undergo conformational changes, adopting in sequential order the 'open', 'tight' and 'loose' conformation during ATP hydrolysis. During catalysis, one catalytic site passes through all three states, while at any time each catalytic site is in a different state than the other two [3,9]. These changes are induced by 'docking-undocking' steps of the γ-subunits to the three different αβ-pairs, i.e. by a rotation of the γ-subunit in the centre of $\alpha_3\beta_3$. At the non-catalytic binding sites, ATP is bound with a $K_d = 25$ μM in the presence of Mg^{2+}, but not hydrolysed [11].

ATP hydrolysis can be observed adding substoichiometric amounts of ATP to the enzyme. In this case, only one catalytic site is occupied and one can observe tight substrate binding with a very slow rate of ATP hydrolysis (unisite ATP hydrolysis conditions). A K_d of <1 nM has been determined for binding ATP at the first site [10,11]. Incubating the enzyme with an excess of ATP allows nucleotide binding to the other sites with a lower affinity. The K_d for the second and third site is approximately 1 and 30 μM, respectively [11]. If all sites are occupied, the rate of ATP

* Corresponding author. Tel.: +49-761-203-6191; fax: +49-761-203-6189.
E-mail address: peter.graeber@physchem.uni-freiburg.de (P. Gräber).

1567-5394/$ - see front matter © 2004 Elsevier B.V. All rights reserved.
doi:10.1016/j.bioelechem.2003.08.008

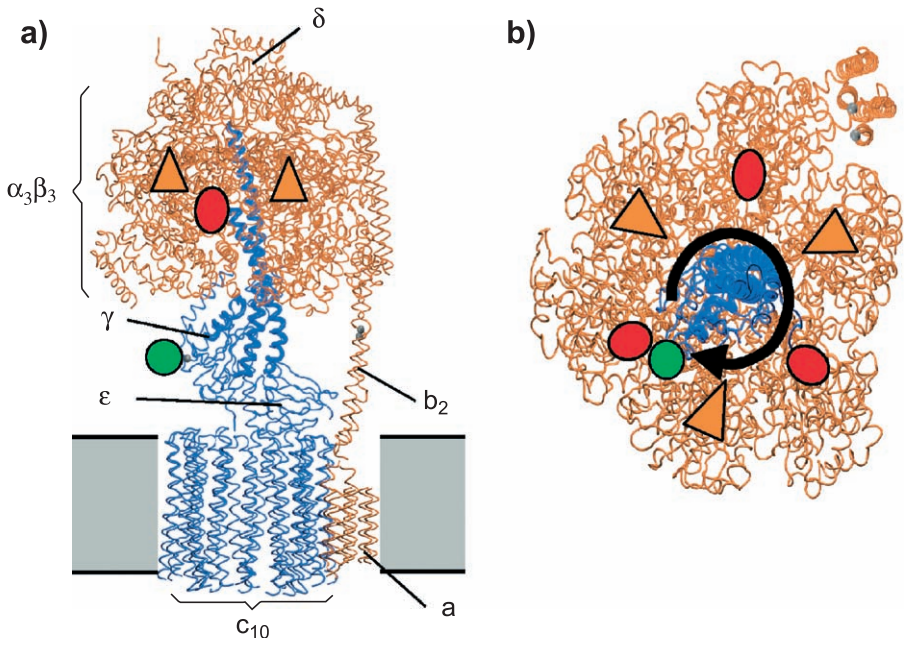

Fig. 1. Model of EF_0F_1 from *E. coli* based on Ref. [26]. (a) Side view. The FRET donor is attached to the γ-subunit at Cys 106 (green circle). Nucleotides in non-catalytic binding sites are shown in orange triangles; nucleotides in catalytic binding sites are shown in red ellipses. The lipid membrane is indicated in grey with black borders. 'Rotor' subunits are blue; 'stator' subunits are orange. (b) Cross section at the level of the nucleotide binding sites, view from top of F_1 in direction to F_0. Orange triangles indicate the non-catalytic binding sites; red ellipses indicate the catalytic binding sites. The position of the FRET donor TMR at Cys γ106 is indicated by a green circle. The direction of stepwise γ-subunit rotation during hydrolysis is given by the circular arrow.

hydrolysis will increase by a factor of 10^4–10^5 (multisite ATP hydrolysis conditions) [10].

Single-molecule investigations avoid the necessity of synchronising an ensemble of enzymes. Simply counting the different conformations one-by-one as well as measuring the kinetics of conformational changes are the major advantages of the fluorescence resonance energy transfer (FRET) approach, which we have established to monitor rotation of the γ-subunit during ATP synthesis and ATP hydrolysis by single H^+-ATP synthases [12,13]. Recently, we showed that adenosine 5′-triphosphate, BODIPY®FL 2′-(or-3′)-*O*-(*N*-(2-aminoethyl)urethane) (BODIPY®FL ATP) and adenosine 5′-triphosphate, BODIPY®TR 2′-(or-3′)-*O*-(*N*-(2-aminoethyl) urethane) (BODIPY®TR ATP) can be hydrolysed by EF_1 at low rates [14].

In this work, we used single-molecule FRET to investigate nucleotide binding to the different binding sites and conformational changes of the enzyme during ATP hydrolysis. To observe the binding of single nucleotides, we incorporated the holoenzyme F_0F_1 into liposomes and labelled specifically the γ-subunit with the FRET donor fluorophore tetramethylrhodamine (TMR). As the FRET acceptor, we used ATP-Alexa Fluor 647. Both labels are small enough to allow ATP binding and an unconstrained catalytic reaction. Using confocal single-molecule fluorescence detection, diffusion of the liposome-bound enzyme through the confocal volume was detected by the donor fluorescence (without acceptor), while binding of a single ATP-Alexa Fluor 647 molecule to a single EF_0F_1 resulted in an intermolecular FRET.

2. Materials and methods

Isolation of the H^+-ATP synthase from *E. coli* (F_1-parts and F_0F_1) were carried out as described earlier [15,16]. TMR-maleimide and ATP-Alexa Fluor 647 were obtained from Molecular Probes (Leiden, The Netherlands). EF_1-γT106C was selectively labelled with TMR in 50 mM MOPS/NaOH (pH 7.0) as described previously [12,17,18]. The labelling reaction was performed at 0 °C. Unbound dye was removed after 5 min by passing twice through Sephadex G50 fine centrifuge columns. Specificity of γ-subunit labelling was checked by fluorescence detection of SDS-PAGE-gels. EF_1-γT106C-TMR concentrations were determined by UV absorption using an extinction coefficient $\varepsilon = 205{,}000\ M^{-1}\ cm^{-1}$ at 278 nm for EF_1 and $\varepsilon = 95{,}000\ M^{-1}\ cm^{-1}$ at 557 nm for TMR. Approximately 65% of EF_1 was labelled with TMR (Fig. 2a).

EF_0F_1 was reconstituted in liposomes with a stoichiometry of one EF_0F_1 per liposome at a concentration of 15 nM [16]. F_1-parts of these enzymes were removed and the remaining F_0-parts in liposomes were reassembled with EF_1-γT106C-TMR to yield liposomes with donor labelled enzymes [12]. Excess EF_1-γT106C-TMR was removed by ultracentrifugation. The efficiency of removing EF_1 and reassembling with EF_1-γT106C-TMR was controlled by measuring ATP synthesis and ATP hydrolysis rates at 23 °C [16].

Fluorescence lifetime of ATP-Alexa Fluor 647 (free and bound to unlabelled EF_1) in buffer A (50 mM HEPES/NaOH, 2.5 mM $MgCl_2$, 400 μM sodium ascorbate, pH 8.0)

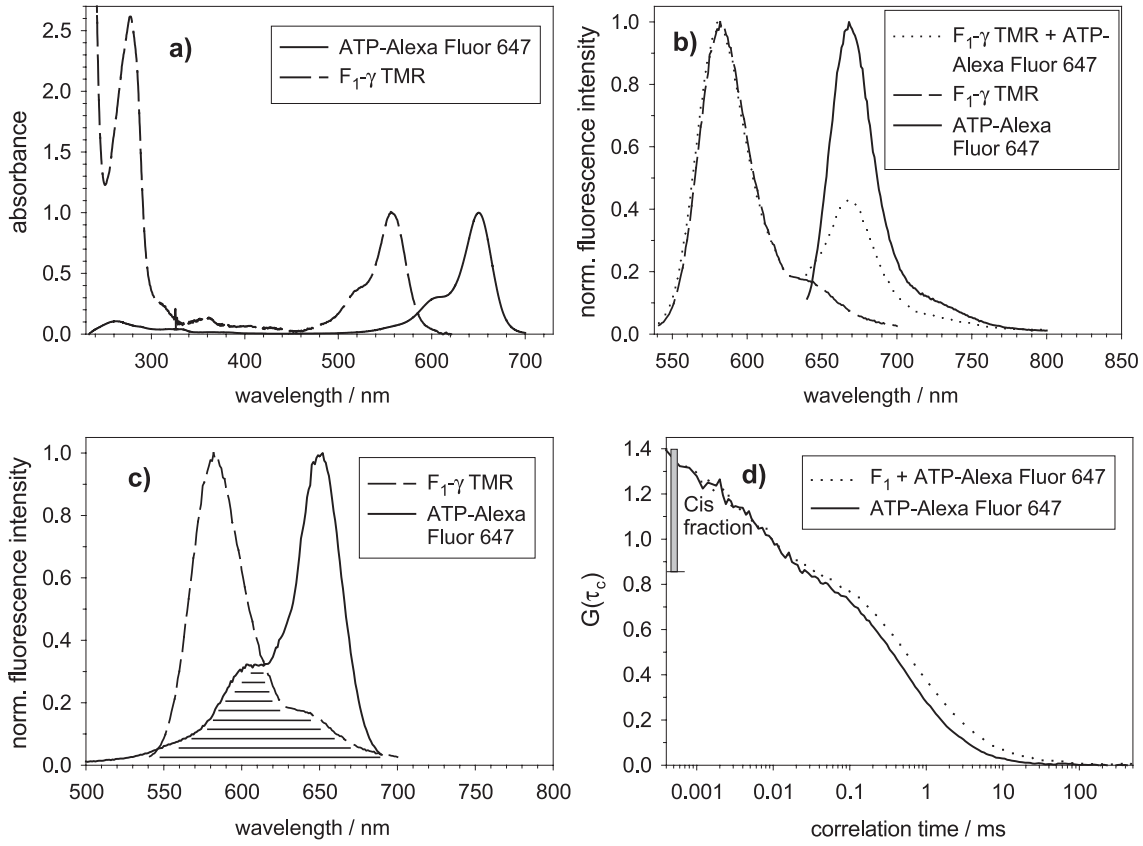

Fig. 2. (a) UV-VIS absorbance spectra of F_1-γTMR-ATPase (1.5 μM) and ATP-Alexa Fluor 647 (2.4 μM) in buffer A. (b) Normalised fluorescence emission spectra of F_1-γTMR-ATPase (200 nM, excited at 532 nm), ATP-Alexa Fluor 647 bound to F_1-γTMR-ATPase (200 nM, excited at 532 nm) and free ATP-Alexa Fluor 647 (800 nM, excited at 632 nm) in buffer A. (c) Normalised emission spectrum of F_1-γTMR-ATPase (200 nM, excited at 532 nm) and absorbance spectrum of ATP-Alexa Fluor 647 (2.4 μM). Spectral overlap of these two curves is shown in the diagram (dashed area). (d) Fluorescence autocorrelation of free ATP-Alexa Fluor 647 and ATP-Alexa Fluor 647 bound to F_1. The two correlation functions $G(\tau_c)$ show different translational diffusion correlation times. In addition below correlation times of 100 μs, a relaxation process can be seen which is due to a photo-induced *cis*–*trans*-isomerisation within in the ATP-Alexa Fluor 647 dye. Approximately 40% of the fluorophores are in the non-fluorescent *cis*-conformation.

was determined by time-correlated single photon counting measurements using a picosecond-pulsed laser diode at 631 nm (FT 200, Picoquant, Berlin, Germany). Single photons were detected at 726 nm. Steady-state fluorescence excitation and emission spectra were measured with an SLM 8100 spectrofluorometer and corrected for wavelength-dependent lamp intensity (Fig. 2b,c).

Diffusion times of ATP-Alexa Fluor 647 (free and bound to unlabelled EF_1) were measured by fluorescence correlation spectroscopy (FCS). Unlabelled F_1-parts (9.7 μM) were mixed with 30 μM ATP-Alexa Fluor 647 and unbound ATP was removed after 10 min by passing through two consecutive Sephadex G50 fine centrifuge columns. Fluorescent samples were diluted to a final concentration of 1 nM in buffer A and were measured immediately at 23 °C in a microscope based confocal set-up using a 635-nm laser-diode (Picoquant) reflected by a dichroic mirror (660 Q, AHF, Tübingen, Germany) and focussed by a water-immersion objective (UplanApo 60 ×, N.A. 1.2, Olympus). Fluorescence photons collected by the same objective were detected by an avalanche photodiode (SPCM AQR 15, EG&G, Canada) passing a 85-μm pinhole and an interference filter HQ 690/60 (AHF). Photons were autocorrelated by a hardware correlator (PC-card ALV5000e/FAST, ALV, Germany).

A confocal set-up of local design was used for the single-molecule detection of freely diffusing, liposome-bound EF_0F_1. Continuous wave excitation was performed by a frequency-doubled Nd:YAG laser (532 nm, Coherent, Germany) attenuated to 70 μW and focussed into the buffer solution by a water immersion objective (UAPO 40 ×, N.A. 1.15, Olympus). Out-of-focus fluorescence was blocked by a 100-μm pinhole (OWIS, Staufen, Germany). Single photons were detected in two spectral regions with two avalanche photodiodes (SPCM AQR 15) after passing an interference filter HQ 575/65 nm (AHF) for TMR and HQ 665 LP (AHF) for ATP-Alexa Fluor 647. Photons in the donor channel (I_{do}) and the acceptor channel (I_{ac}) were registered simultaneously with a multi-channel scaler (MCS-card PMS 300, Becker and Hickl, Berlin, Germany) set to 1-ms time bins per channel. Analysis of the two-channel MCS traces was performed with the program 'burstanalyzer' written by N. Zarrabi (3. Physikalisches Institut, Universität Stuttgart, Germany). From the fluores-

cence intensity traces, the proximity factors $P = I_{ac}/(I_{do} + I_{ac})$ were calculated and FRET efficiencies classified.

For single-molecule detection, the donor-labelled EF_0F_1 embedded in liposomes were incubated stoichiometrically with ATP-Alexa Fluor 647 in buffer A and diluted to a final concentration of approximately 100 pM in order to detect only one liposome in the confocal volume at any time. Measurements were performed in buffer A at 23 °C after removal of fluorescent impurities of the buffer by activated charcoal [17].

3. Results

F_1-parts of the H^+-ATP synthase of *E. coli* were labelled specifically at the γ-subunit with TMR-maleimide and specificity was checked by SDS-PAGE (data not shown). The labelling efficiency was approximately 65%. EF_1-γT106C-TMR were reassembled with membrane-integrated F_0-parts to yield a fully functional holoenzyme F_0F_1 in liposomes. The turnovers of the enzyme measured under standard conditions at 23 °C [15] were $(78 \pm 5)\ s^{-1}$ for ATP synthesis and $(186 \pm 12)\ s^{-1}$ for ATP hydrolysis, and they decreased to $(42 \pm 10)\ s^{-1}$ for ATP synthesis and $(79 \pm 14)\ s^{-1}$ for ATP hydrolysis after removal of F_1 and reassembling of EF_1-γT106C-TMR.

In order to observe binding of ATP to the enzyme by FRET, we used the fluorescent derivative ATP-Alexa Fluor 647, where the fluorophore is linked to the ribose of ATP. The spectroscopic properties of the FRET pair EF_1-γT106C-TMR (donor) and ATP-Alexa Fluor 647 (acceptor) are shown in Fig. 2. Fig. 2a shows the absorbance spectra of both fluorophores; Fig. 2b the fluorescence emission spectra of both fluorophores and in addition the spectrum of ATP-Alexa Fluor 647 bound to EF_1-γT106C-TMR. Binding was accomplished by incubating 200 nM of EF_1-γT106C-TMR for 10 min at 23 °C with 200 nM of ATP-Alexa Fluor 647 in buffer A. It can be seen that excitation of the FRET donor EF_1-γT106C-TMR at 532 nm yielded fluorescence emission of ATP-Alexa Fluor 647 with a maximum at 665 nm. The spectral overlap of the emission spectrum of EF_1-γT106C-TMR with the absorbance spectrum of ATP-Alexa Fluor 647 in buffer A is shown in Fig. 2c (dashed area).

The diffusion of free ATP-Alexa Fluor 647 and F_1-bound ATP-Alexa Fluor 647 was investigated with FCS. Fig. 2d shows the autocorrelation functions $G(\tau_c)$ [17]. By fitting these data, we obtained translational diffusion correlation times of 0.49 ms for free ATP-Alexa Fluor 647 and 2.3 ms for F_1-bound ATP-Alexa Fluor 647 (solution contained approximately 30% of free ATP-Alexa Fluor 647 or ADP-Alexa Fluor 647). The increase of the diffusion correlation time is due to the large increase in the mass of the diffusing particle, when ATP-Alexa Fluor 647 is bound to F_1. It should be mentioned that, below correlation times of 100 μs, the autocorrelation function indicates, presumably, a photoinduced *cis–trans*-isomerisation in ATP-Alexa Fluor 647, similar as it has been reported for the fluorophore Cy5 [19,20]. Excited with 100 μW, the fraction of the non-fluorescent *cis*-state of the fluorophores reached 40%. In addition, we determined the fluorescence lifetime of ATP-Alexa Fluor 647 to $\tau = (1.37 \pm 0.08)$ ns in buffer A and to $\tau = (1.42 \pm 0.09)$ ns after its binding to non-labelled F_1-parts.

Using TMR-labelled F_0F_1-ATP synthases reconstituted in liposomes as donor and ATP-Alexa Fluor 647 as acceptor, intermolecular FRET was measured with single enzymes in a confocal set-up with two-channel detection. Photons from TMR were detected in the spectral range of 545–610 nm near its fluorescence maximum and from Alexa Fluor 647 at wavelengths above 665 nm. Well-separated photon burst with count rates up to 120 photons per ms were observed, when a single liposome with one TMR-labelled F_0F_1-ATP synthase diffused through the detection volume (Fig. 3). When a single ATP-Alexa Fluor 647 diffused through the detection volume, no photons could be detected because the FRET acceptor was not excited directly at the applied laser wavelength and intensity. As the enzyme contains three catalytic and three non-catalytic binding sites (Fig. 1b), conditions were chosen which ensure that only one ATP-Alexa Fluor 647 is bound per enzyme. Binding of ATP-Alexa Fluor 647 to the TMR-labelled H^+-ATP synthase in liposomes led to an intermolecular FRET, i.e. photons in both the donor and the acceptor channel are detected.

FRET efficiencies E can be calculated according to $E = 1/[1 + \gamma(I_{do}/I_{ac})]$, where I_{do} and I_{ac} are the measured fluorescence intensities of the donor and acceptor, and γ is a factor that corrects the detection efficiencies and fluorescence quantum yields [21,22]. If γ is assumed to be about 1, the equation corresponds to the proximity factor $P = I_{ac}/(I_{do} + I_{ac})$, which is used in the following. This approximation leads to the effect that the donor-only trace (DO in Fig. 3f–h) shows a proximity factor of 0.1.

We estimated the FRET efficiencies for all single-enzyme photon bursts by calculating the proximity factor P. In the presence of ATP-Alexa Fluor 647, photon bursts with different proximity factors, i.e. FRET states were observed (Fig. 3a–e). In Fig. 3a, only the background signal in both channels is seen until at 900 ms. At this time, a liposome enters the detection volume and the TMR fluorescence intensity (green trace) increases to approximately 100 counts/ms. Simultaneously, the Alexa Fluor 647 intensity (red trace) increases to a maximum of approximately 25 counts/ms. At 980 ms, the liposome leaves the detection volume and fluorescence in both channels decreases to the background level. The proximity factor trace, shown in the upper part of the diagram, remained at a constant level throughout the burst.

In the confocal volume, a three-dimensional Gaussian intensity distribution for excitation and detection can be observed. Time-dependent fluctuations in the fluorescence intensities in both channels were due to the diffusion of the liposome through this confocal volume. However, the ratiometric proximity factor P is expected to be independent

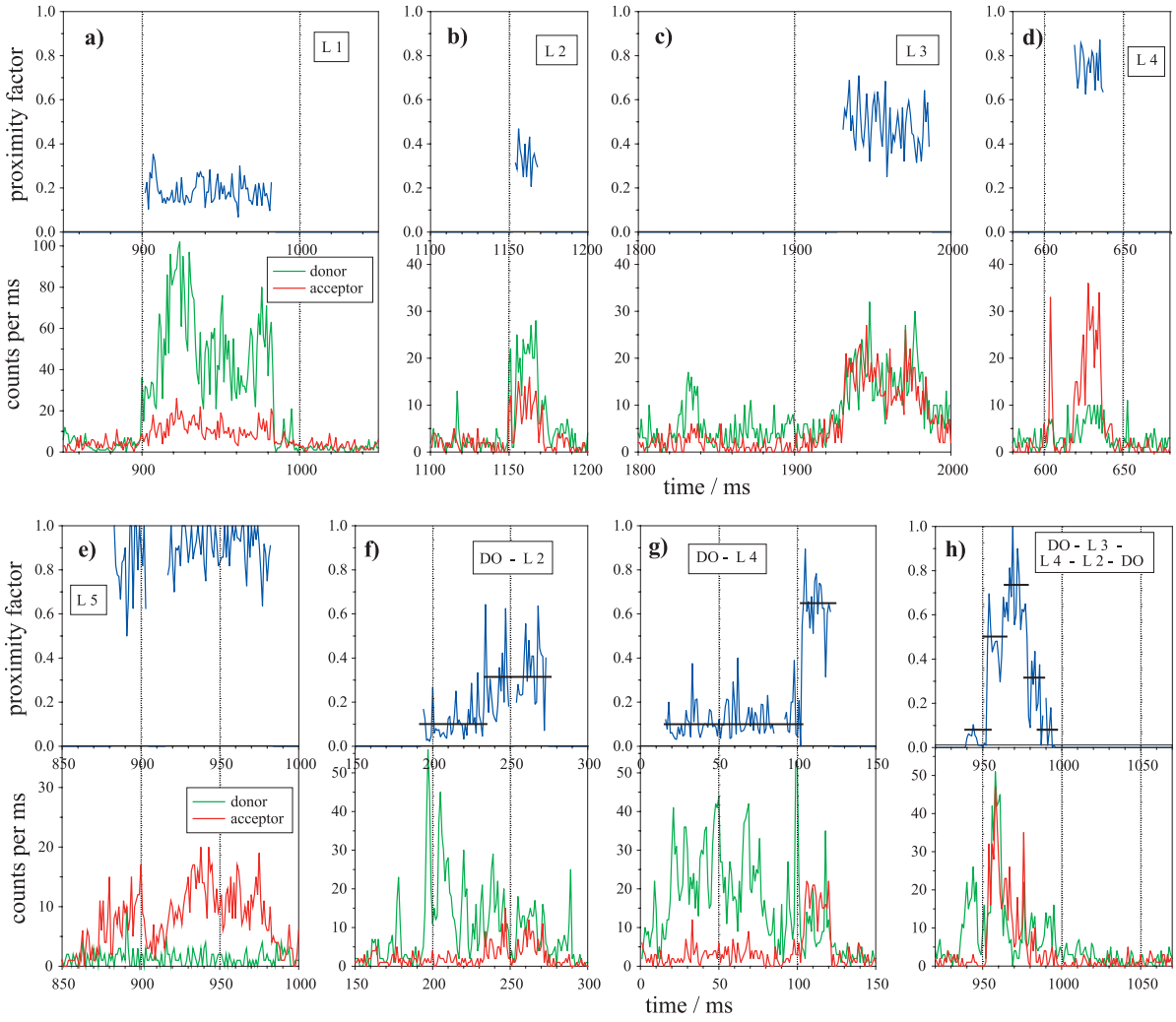

Fig. 3. Photon bursts (green: donor channel, red: acceptor channel) and proximity factor traces (blue curves) of single TMR-labelled F_0F_1-ATP synthases in liposomes. Single-molecule fluorescence of TMR-labelled F_0F_1-ATP synthases in liposomes is observed when liposomes containing one enzyme traverse the confocal detection volume. (a–e) Enzyme-bound ATP-Alexa Fluor 647 to F_0F_1 results in five different FRET efficiencies where the proximity factor remains constant during the burst. (f and g) Nucleotide binding is observed as a sudden jump in the proximity factor trace within the photon burst from a donor-only level (DO) to L2 (f) and L4 (g), respectively. (h) Addition of 0.15 μM ATP to a mixture of F_0F_1-ATP synthase (150 pM) and ATP-Alexa Fluor 647 (125 pM) leads to fluctuations of the proximity factor trace within a single photon burst.

of the location, i.e. it should remain constant. Photon bursts were classified according to their proximity factor into five distinct classes, two 'low FRET' states (L1 and L2), one 'medium FRET' state (L3) and two 'high FRET' states (L4 and L5). Examples of these five states are shown in this order in Fig. 3a–e.

Single-molecule detection of organic molecules is time limited as a fluorophore undergoes photobleaching after approximately 10^5–10^6 excitation cycles in the focus [22]. Photobleaching of the acceptor-fluorophore could be observed within some bursts (data not shown), indicated by a spontaneous decrease of the acceptor count rate to the background level, accompanied by a simultaneous rise of the donor count rate. Such events could be seen for all FRET levels. This indicates that in every FRET state only one ATP-Alexa Fluor 647 is bound to the enzyme.

Nucleotide binding events could be observed directly as shown in Fig. 3f and g. A sudden jump in the proximity factor trace within the photon burst from a donor-only level (DO) to L2 (Fig. 3f) and L4 (Fig. 3g), respectively, was caused by the spontaneous increase in the photon count rate of the acceptor channel and a parallel decrease in the donor channel. The different proximity factors observed in Fig. 3f and g indicate that binding of the ATP-Alexa Fluor 647 occurs to binding sites with different distances to TMR at the γ-subunit.

Upon addition of a 0.15 μM ATP to a pre-incubated mixture of F_0F_1-ATP synthase (150 pM) and ATP-Alexa Fluor 647 (125 pM), fluctuations of the proximity factors within a single photon burst could be observed. In Fig. 3h, a burst is shown where binding of ATP-Alexa Fluor 647 (DO → L3) is followed by two further jumps to FRET

levels L4 and L2 before the signal returns to DO. The overall sequence is DO → L3 → L4 → L2 → DO.

4. Discussion

In this work, we investigated the feasibility to observe binding of a single nucleotide to a single membrane-integrated H^+-ATP synthase. We developed an intermolecular FRET approach using ATP-Alexa Fluor 647 as FRET acceptor. The FRET donor TMR was covalently attached to the γ-subunit of H^+-ATP synthase. Binding of the ATP analogue to F_1 was shown by FCS, indicated by prolonged diffusion times as compared to the unbound nucleotide. After binding of ATP-Alexa Fluor 647 to TMR-labelled F_1-parts, FRET was detected in the static fluorescence spectra. The fluorescence properties of ATP-Alexa Fluor 647 changed not significantly after binding as indicated by fluorescence spectra and lifetimes.

Two-channel photon detection allowed the registration of the fluorescence of the donor and acceptor during the transit of a single FRET pair through the confocal volume. Binding of a single ATP-Alexa Fluor 647 to a single liposome-bound F_0F_1-ATP synthase was measured by intermolecular FRET at low ATP concentrations (unisite conditions for ATP hydrolysis). We classified five different FRET states according to their proximity factors. This result can be explained assuming five different distances between the reference position at the γ-subunit and the binding site. At unisite conditions, all distances remained constant within one photon burst, excluding a fast rotary motion of the γ-subunit during the transit of the FRET pair through the detection volume. As shown in Fig. 1, the maximum number of possible distances is six, if all three catalytic and three non-catalytic binding site are likely to bind ATP-Alexa Fluor 647. There are several possibilities, which result in five distances: one nucleotide-binding site is always occupied (e.g. an ATP at a non-catalytic binding site). We prepared our samples as described in Ref. [23], which results in a nucleotide-depleted EF_1. Nevertheless, during the preparation of F_1, 1 mM ATP was added for stability reasons. Therefore, we cannot exclude that one site still is occupied with a nucleotide.

Another possibility is that the distances of two binding sites relative to TMR at γT106C are very similar that they could not be distinguished by FRET. Alternatively, ATP-Alexa Fluor 647 binds only to catalytic sites. In this case, we must consider that binding of ATP and ATP hydrolysis leads to substeps within a 120° rotation for low ATP concentrations as reported recently [24,25]. In this case, also six different FRET levels are expected. However, two of these distances might be very similar as they do not result in different FRET states.

Recently, we have shown that other ATP analogues, similar to ATP-Alexa Fluor 647, are hydrolysed under multisite ATP hydrolysis conditions [14]. Taken this as a hint, we might expect binding of ATP-Alexa Fluor 647 to all three catalytic sites. The binding process and its kinetics is seen by the sudden jumps in the proximity factor (Fig. 3f,g) and, obviously, binding occurs to different sites which are characterised by their different energy transfer efficiencies to the donor at the γ-subunit.

The position of the γ-subunit within the $\alpha_3\beta_3$-complex determines, presumably, the affinity of the three nucleotide binding sites. At a substoichiometric ratio, i.e. less than one ATP per enzyme, it is expected that mainly the site with the highest affinity is occupied and consequently, one FRET state should be observed preferentially. However, five different FRET states are detected implying that binding to further sites was observed. In a preliminary proximity factor histogram, the L1 level seemed to be preferred but the number of analysed events is yet too small to allow a general statement on the distribution of FRET states.

Multisite hydrolysis conditions were achieved upon addition of excess ATP to H^+-ATP synthase with bound ATP-Alexa Fluor 647. Stepwise changes of the proximity factor indicated stepwise changes in the distances between the single FRET pair. The duration of each FRET state (Fig. 3h) is short due to fast multisite ATP hydrolysis as compared to ATP hydrolysis at unisite conditions. This trace can be interpreted in two ways: when ATP-Alexa Fluor 647 is bound to a non-catalytic site, it remains bound at this site during the complete ATP hydrolysis cycle which involves only the catalytic sites and which requires three different positions of the γ-subunit relative to the ATP-Alexa Fluor 647 at the non-catalytic sites. If ATP-Alexa Fluor 647 was bound to a catalytic site we could observe a binding step resulting immediately in a jump from DO to FRET level L3, and then two further jumps to FRET levels L4 and L2, before the signal returned to the starting level when the nucleotide is released from the enzyme. This might indicate, that the fluorescent nucleotide had to remain on the site until two additional ATP were hydrolysed. This observation might support a tri-site mechanism of ATP hydrolysis, where three nucleotides have to be present at any time to achieve maximum rates of catalysis.

In this work, we showed that binding of single nucleotides to the H^+-ATP synthase and hydrolysis can be observed on a single-molecule level with an intermolecular FRET approach. This seems to be a promising method to resolve mechanistic questions of catalysis.

Acknowledgements

We thank R.A. Capaldi and R. Aggeler for the gift of the γ-mutant and T. Steinbrecher for his help. S. Steigmiller is supported by a fellowship of the Studienstiftung des deutschen Volkes (Bonn, Germany). B. Zimmermann gratefully acknowledges financial support by the Landesstiftung Baden-Württemberg (Stuttgart, Germany) in the project ‘functional nanodevices’.

References

[1] R.A. Capaldi, R. Aggeler, Mechanism of the F_1F_0-type ATP synthase, a biological rotary motor, Trends Biochem. Sci. 27 (2002) 154–160.

[2] A.E. Senior, S. Nadanaciva, J. Weber, The molecular mechanism of ATP synthesis by F_1F_0-ATP synthase, Biochim. Biophys. Acta 1553 (2002) 188–211.

[3] P.D. Boyer, ATP synthase—past and future, Biochim. Biophys. Acta 1365 (1998) 3–9.

[4] M. Yoshida, E. Muneyuki, T. Hisabori, ATP synthase—a marvelous rotary engine of the cell, Nat. Rev., Mol. Cell Biol. 2 (2001) 669–677.

[5] D. Stock, A.G.W. Leslie, J.E. Walker, Molecular architecture of the rotary motor in ATP synthase, Science 286 (1999) 1700–1705.

[6] B. Böttcher, L. Schwarz, P. Gräber, Direct indication for the existence of a double stalk in CF_0F_1, J. Mol. Biol. 281 (1998) 757–762.

[7] S. Karrasch, J.E. Walker, Novel features in the structure of bovine ATP synthase, J. Mol. Biol. 290 (1999) 379–384.

[8] S. Wilkens, R.A. Capaldi, Electron microscopic evidence of two stalks linking the F_1 and F_0 parts of the *Escherichia coli* ATP synthase, Biochim. Biophys. Acta 1365 (1998) 93–97.

[9] P.D. Boyer, The binding change mechanism for ATP synthase—some probabilities and possibilities, Biochim. Biophys. Acta 1140 (1993) 215–250.

[10] H.S. Penefsky, Rate constants and equilibrium constants for the elementary steps of ATP hydrolysis by beef heart mitochondrial ATPase, Methods Enzymol. 126 (1986) 608–618.

[11] J. Weber, A.E. Senior, Catalytic mechanism of F_1-ATPase, Biochim. Biophys. Acta 1319 (1997) 19–58.

[12] M. Börsch, M. Diez, B. Zimmermann, R. Reuter, P. Gräber, Stepwise rotation of the γ-subunit of EF_0F_1-ATP synthase observed by intramolecular single-molecule fluorescence resonance energy transfer, FEBS Lett. 527 (2002) 147–152.

[13] M. Diez, B. Zimmermann, M. Börsch, M. König, E. Schweinberger, S. Steigmiller, R. Reuter, S. Felekyan, V. Kudryavtsev, C.A.M. Seidel, P. Gräber, Proton-powered subunit rotation in single membrane-bound F0F1-ATP synthase, Nature Struct. Biol. 11 (2004) 135–141.

[14] T. Steinbrecher, O. Hucke, S. Steigmiller, M. Börsch, A. Labahn, Binding affinities and protein ligand complex geometries of nucleotides at the F_1 part of the mitochondrial ATP synthase obtained by ligand docking calculations, FEBS Lett. 530 (2002) 99–103.

[15] S. Fischer, P. Gräber, Comparison of ΔpH- and ΔΦ-driven ATP synthesis catalyzed by the H^+-ATPases from *Escherichia coli* or chloroplasts reconstituted in liposomes, FEBS Lett. 457 (1999) 327–332.

[16] S. Fischer, P. Gräber, P. Turina, The activity of the ATP synthase from *Escherichia coli* is regulated by the transmembrane proton motive force, J. Biol. Chem. 275 (2000) 30157–30162.

[17] M. Börsch, P. Turina, C. Eggeling, J.R. Fries, C.A.M. Seidel, A. Labahn, P. Gräber, Conformational changes of the H^+ATPase from *Escherichia coli* upon nucleotide binding detected by single molecule fluorescence, FEBS Lett. 437 (1998) 251–254.

[18] P. Turina, R.A. Capaldi, ATP hydrolysis-driven structural changes in the gamma-subunit of *Escherichia coli* ATPase monitored by fluorescence from probes bound at introduced cysteine residues, J. Biol. Chem. 269 (1994) 13465–13471.

[19] J. Widengren, P. Schwille, Characterization of photoinduced isomerization and back-isomerization of the cyanine dye Cy5 by fluorescence correlation spectroscopy, J. Phys. Chem., A Mol. Spectrosc. Kinet. Environ. Gen. Theory 104 (2000) 6416–6428.

[20] J. Widengren, C.A.M. Seidel, Manipulation and characterization of photo-induced states of merocyanine 540 by fluorescence correlation spectroscopy, Phys. Chem. Chem. Phys. 2 (2000) 3435–3441.

[21] S. Weiss, Fluorescence spectroscopy of single biomolecules, Science 283 (1999) 1676–1683.

[22] A.A. Deniz, T.A. Laurence, M. Dahan, D.S. Chemla, P.G. Schultz, S. Weiss, Ratiometric single-molecule studies of freely diffusing biomolecules, Annu. Rev. Phys. Chem. 52 (2001) 233–253.

[23] H.S. Penefsky, Reversible binding of P_i by beef heart mitochondrial adenosine triphosphatase, J. Biol. Chem. 252 (1977) 2891–2899.

[24] R. Yasuda, H. Noji, M. Yoshida, K.J. Kinosita, H. Itoh, Resolution of distinct rotational substeps by submillisecond kinetic analysis of F_1-ATPase, Nature 410 (2001) 898–904.

[25] R. Yasuda, T. Masaike, K. Adachi, H. Noji, H. Itoh, K.J. Kinosita, The ATP-waiting conformation of rotating F_1-ATPase revealed by single-pair fluorescence resonance energy transfer, Proc. Natl. Acad. Sci. U. S. A. 100 (2003) 9314–9318.

[26] S. Engelbrecht, W. Junge, ATP synthase: a tentative structural model, FEBS Lett. 414 (1997) 485–491.